Journal of Sound and Vibration 332 (2013) 6078–6092

Contents lists available at ScienceDirect

Journal of Sound and Vibration

journal homepage: www.elsevier.com/locate/jsvi

Closed-form solutions for non-uniform Euler–Bernoulli free–free beams

Korak Sarkar, Ranjan Ganguli *

Department of Aerospace Engineering, Indian Institute of Science, Bangalore 560012, India

ARTICLE INFO

Article history:
Received 22 November 2012
Received in revised form
4 June 2013
Accepted 7 June 2013
Handling Editor: L.G. Tham
Available online 22 July 2013

ABSTRACT

In this paper, the free vibration of a non-uniform free–free Euler–Bernoulli beam is studied using an inverse problem approach. It is found that the fourth-order governing differential equation for such beams possess a fundamental closed-form solution for certain polynomial variations of the mass and stiffness. An infinite number of non-uniform free–free beams exist, with different mass and stiffness variations, but sharing the same fundamental frequency. A detailed study is conducted for linear, quadratic and cubic variations of mass, and on how to pre-select the internal nodes such that the closed-form solutions exist for the three cases. A special case is also considered where, at the internal nodes, external elastic constraints are present. The derived results are provided as benchmark solutions for the validation of non-uniform free–free beam numerical codes.

© 2013 Elsevier Ltd. All rights reserved.

1. Introduction

Non-uniform free–free Euler–Bernoulli beam is used to mathematically model many important mechanical, aerospace and naval engineering structures such as aircrafts, missiles [1–3], rockets [4], ships [5], and baseball bats [6,7]. In recent years, free–free beams have also been used in the MEMS industry as mechanical resonators [8–10]. So the vibration analysis of the free–free beam is very important from a structural dynamics point of view. The non-uniform Euler–Bernoulli beam is governed by a fourth-order differential equation which does not yield a simple closed-form solution, unlike its uniform counterpart. But closed-form solutions in vibration analysis have always played an important role in structural dynamics [11–14], which does not exist for non-uniform free–free beams. Based on the applications point of view, considerable research has been done on the subject of free–free beams.

Mermagen and Murphy [2] studied the flight mechanics of an elastic symmetric missile. They stated that the free-flight motion of an elastic missile is approximated by three bodies connected by two mass-less cantilever beams. If the mass distribution of the three bodies is 1–2–1, the frequency of symmetric oscillation of the outer bodies is within 5 percent of the classical frequency of oscillation of a free–free beam. Pradhan and Datta [3] studied the effect of rocket mass and an intermediate mass on the critical flutter load of a free–free beam using a finite element model considering shear deformation and rotary inertia based on Hamilton's principle applied to non-conservative systems. Ohshima and Sugiyama [4] also studied the dynamic stability of a flexible rocket body accommodated by heavy payload at its nose, where they assume that the end rocket thrust acts as follower/non-conservative load on the flexible rocket body. The rocket is simplified as a uniform free–free beam with spherical mass at the nose.

* Corresponding author. Tel.: +91 80 2293 3017; fax: 91 80 2360 0134.
E-mail addresses: koraksarkar@aero.iisc.ernet.in (K. Sarkar), ganguli@aero.iisc.ernet.in (R. Ganguli).

0022-460X/$ - see front matter © 2013 Elsevier Ltd. All rights reserved.
http://dx.doi.org/10.1016/j.jsv.2013.06.008

Wu and Ho [5] studied the natural frequencies and mode-shapes of the horizontal and torsion coupled vibration of a ship hull using a finite element method, the dynamic behaviour of a ship hull due to the excitation of regular waves was analysed by means of the Newmark direct integration method. In order to properly determine the property matrices the hull was considered as a non-uniform free–free beam composed of various open and closed wall thin sections. Brody [7] showed that a hand-held baseball bat oscillates in the first elastic mode of a free–free beam when it strikes a ball. He also showed that one of the "sweet spots" of a baseball bat lies at one of the nodal points of the fundamental elastic mode of the free–free beam [6]. Since the vibrational motion of the bat is very small in this region, an impact in this region will result in very little vibration of the bat and maximum energy being delivered to the baseball.

Wang et al. [8] designed free–free beam flexural-mode micro-mechanical resonators utilising non-intrusive supports. The device comprises a uniform free–free beam supported at its flexural nodal points by four torsional beams which are strategically designed with quarter-wavelength dimensions, so as to effect an impedance transformation that isolates the free–free beam from rigid anchors. The resonator operates as if levitated without any support and hence is proposed as a better choice over its clamped–clamped counterparts. When a large voltage is applied between the electrode and the resonator, the whole structure comes down and rests upon dimples which are located at flexural node points of the fundamental elastic mode, and thus, does not have any impact on the resonator operation. Demirci and Nyugen [9] carried out similar studies for polysilicon free–free beam micro-mechanical resonators based on MEMS technology operating in the second and third mode flexural vibration. Davis et al. [10] presented the design, fabrication and preliminary characterisation of a novel MEMS based resonator based on a uniform free–free beam. The resonator is anchored at the nodal locations of the fundamental elastic mode in order to quench the dominant spurious mode and is excited by means of an electrode buried on the surface. The above studies clearly show the importance of nodal positions in the design of free–free MEMS resonators.

The available literature for the vibration analysis of non-uniform free–free beams is very limited. Naguleswaran [15] presented a direct analytical solution for mode shape equation for vibration analysis of a homogeneous Euler–Bernoulli beam of constant depth and linearly varying breadth. He presented the solutions for a free–free beam, for both pointed end and truncated edge, based on the Frobenius method of series solution of differential equations. He performed similar studies for wedge and cone beams to derive analytical solutions for mode shape equations based on Bessel functions, and derived the results for free–free beam [16]. Zhou and Cheung [17] studied the vibrational characteristics of tapered Euler–Bernoulli beam, with free–free beam as one of the boundary conditions, with continuously varying rectangular cross-section using the Taylor series expansion and Rayleigh–Ritz method.

Most of these studies deal with approximate and numerical methods for the study of non-uniform Euler–Bernoulli beams. For all practical purposes, these methods give fairly accurate results. So why do we still look for closed-form solutions? It is because, these closed-form solutions provide benchmark solutions for the validation of the numerical and approximate methods. Caddemi and Calio [11] proposed a suitable procedure for exact integration of the governing equation of the mode shapes in the presence of singularities in flexural stiffness, representing concentrated cracks which is of great help to researchers working towards the evaluation of the dynamic response of structures composed of damaged beams. Stojanovic et al. [12] presented explicit analytical expression for the natural frequencies and critical buckling load using trigonometric method. Rusin et al. [13] presented a part of the classical solution of the response of a double-string system subjected to a force moving with constant velocity in a closed, analytical form.

Elishakoff and Candan [18] were the first to find the closed-form solutions for inhomogeneous Euler–Bernoulli beams under different boundary conditions using the inverse problem approach. Elishakoff and his coauthors have consistently used the inverse problem approach for a wide variety of vibration problems [19–26]. Closed-form solutions have been also provided by making use of both exponential and trigonometric functions [27–30]. But they have not provided closed-form solutions for the non-uniform free–free beam problem. This is the main motivation behind the current work. The fundamental mode of a non-uniform free–free beam has two internal nodes. Elishakoff and Neuringer [31] used the inverse problem approach to study inhomogeneous beams that may possess a prescribed polynomial second mode, where they take an internal node into consideration. This idea has been used in the present work to include two internal nodes for the assumed fundamental mode shape for a non-uniform free–free beam.

In this paper, we assume a prescribed polynomial, having two internal nodes, as the fundamental mode shape which satisfies the boundary conditions of a non-uniform free–free beam. Then we have used the inverse problem approach to show that for certain mass and stiffness distributions of the beam, there exists a simple closed-form solution given by the assumed polynomial. We have also considered a special case where the external elastic constraints are present at the internal node locations. We have used the derived results to check a numerical method used for the vibration analysis of a non-uniform free–free beam. The proposed approach also allows us to design free–free beams with tailored mode shapes and specified nodal locations.

2. Mathematical formulation

The dynamics of a non-uniform Euler–Bernoulli beam is governed by the following fourth-order differential equation [32]:

$$\frac{\partial^2}{\partial x^2}\left(EI(x)\frac{\partial^2 w(x,t)}{\partial x^2}\right)+m(x)\frac{\partial^2 w(x,t)}{\partial t^2}=0 \tag{1}$$

where L is the length of the beam, $EI(x)$ is the flexural rigidity of the beam, $m(x)$ is the mass per unit length, and $w(x,t)$ is the transverse displacement of the beam at a position x, at time t. Considering harmonic vibration, Eq. (1) yields

$$\frac{\partial^2}{\partial x^2}\left(EI(x)\frac{\partial^2\phi(x)}{\partial x^2}\right)-m(x)\omega^2\phi(x)=0 \tag{2}$$

where $\phi(x)$ and ω denote the mode shape and frequency, respectively. We now determine a polynomial function $\phi(x)$ which satisfies the boundary conditions of a free–free beam given by

$$\phi''(0)=0,\quad \phi'''(0)=0,\quad \phi''(L)=0,\quad \phi'''(L)=0 \tag{3}$$

This polynomial function $\phi(x)$ has two internal nodes at $x=\alpha$ $(0<\alpha<L)$ and $x=\beta$ $(0<\beta<L)$, and serves as a mode shape satisfying Eq. (2) with polynomial variations of $m(x)$ and $EI(x)$. We also add the condition $\phi(L)=1$ to normalise the mode shape. The mode shape satisfying the boundary conditions given by Eq. (3) will be sought as a sixth-order polynomial given by

$$\phi(x)=c_0+c_1x+c_2x^2+c_3x^3+c_4x^4+c_5x^5+c_6x^6 \tag{4}$$

Satisfying the boundary conditions, given by Eq. (3), along with imposing the conditions $\phi(\alpha)=0$, $\phi(\beta)=0$ and $\phi(L)=1$, yields a set of linear equations, solving which, we get the following expressions for c_i's:

$$c_0=\frac{\alpha\beta(5L^2(\alpha^2+\alpha\beta+\beta^2)-6L(\alpha^3+\alpha^2\beta+\alpha\beta^2+\beta^3)+2(\alpha^4+\alpha^3\beta+\alpha^2\beta^2+\alpha\beta^3+\beta^4))}{A},$$
$$c_1=\frac{-5L^2(\alpha^3+\alpha^2\beta+\alpha\beta^2+\beta^3)+6L(\alpha^4+\alpha^3\beta+\alpha^2\beta^2+\alpha\beta^3+\beta^4)}{A}$$
$$\frac{-2(\alpha^5+\alpha^4\beta+\alpha^3\beta^2+\alpha^2\beta^3+\alpha\beta^4+\beta^5)}{A},\quad c_2=0,\quad c_3=0,\quad c_4=\frac{5L^2}{A},\quad c_5=-\frac{6L}{A},\quad c_6=\frac{2}{A} \tag{5}$$

where

$$A=(L-\alpha)(L-\beta)(L^4+L^3(\alpha+\beta)+L^2(\alpha^2+\alpha\beta+\beta^2)-4L(\alpha^3+\alpha^2\beta+\alpha\beta^2+\beta^3)+2(\alpha^4+\alpha^3\beta+\alpha^2\beta^2+\alpha\beta^3+\beta^4)) \tag{6}$$

Now we assume that the mass $m(x)$ and stiffness $EI(x)$ variations of the beam are given by simple polynomial functions

$$m(x)=\sum_{i=0}^{p}a_ix^i \tag{7}$$

$$EI(x)=\sum_{i=0}^{q}b_ix^i \tag{8}$$

where p and q are the positive integers, and since the first term in Eq. (2) contains fourth-order derivative, we will restrict our considerations to $q=p+4$. We investigate the class of special problems where the mode shape $\phi(x)$ will be represented by a simple polynomial satisfying all the necessary boundary conditions. First, we will determine the coefficients c_i's such that $\phi(x)$ satisfies the boundary conditions given in Eq. (3). Since the assumed mode shape contains two nodes, it is considered as the fundamental mode shape for the free–free beam vibration. This is the first elastic mode of the free–free beam, which has two rigid body modes. Further, we will determine the mass $m(x)$ and stiffness $EI(x)$ variations such that the fundamental mode shape of the beam's vibration coincides with the assumed polynomial mode shape. We will conduct our analysis with particular cases of linear, quadratic and cubic variations of the mass distribution in Sections 2.1–2.3, respectively.

2.1. Free-free beam with linear mass distribution ($p=1$)

For this case, the mass and stiffness variations for the beam is given by

$$m(x)=a_0+a_1x \tag{9}$$

$$EI(x)=b_0+b_1x+b_2x^2+b_3x^3+b_4x^4+b_5x^5 \tag{10}$$

We put the expressions for $m(x)$ and $EI(x)$, given by Eqs. (9) and (10), and $\phi(x)$, given by Eq. (4), into Eq. (2), resulting in a polynomial equation with the highest term of x^7. For this polynomial equation to be satisfied for all values of x, the coefficients of the constant, x, x^2, x^3, x^4, x^5, x^6 and x^7 must be set to zero. Thus, yielding a set of eight linear homogeneous equations in eight unknowns

$$\mathbf{A}^{(1)}\mathbf{y}^{(1)}=\mathbf{0} \tag{11}$$

where the matrix $\mathbf{A}^{(1)}$ is given by Eq. (A.1) and the vector $\mathbf{y}^{(1)}=\{a_0,a_1,b_0,b_1,b_2,b_3,b_4,b_5\}^T$. Now, in order to have a non-trivial solution, the determinant of matrix $\mathbf{A}^{(1)}$ must be zero, leading to a complicated equation in α, β and ω, of the form $F_1(\alpha,\beta)\omega^4=0$, where F_1 is a complicated polynomial expression in β and α. This means either $F_1(\alpha,\beta)=0$ or $\omega^4=0$. But always fundamental frequency $\omega>0$. Thus, we get

$$F_1(\alpha,\beta)=0 \tag{12}$$

In order to solve Eq. (12), one of the two parameters (α or β) have to specified. In this case, we will assume the value of one of the arbitrary nodes β, and determine the other node α with respect to the specified value. The value of the known node is taken at $x=\beta=0.78L$. Thus, solving Eq. (12) for α, the only real value that we get within the domain $0<\alpha<L$ is $\alpha=0.227596L$. Eq. (12) is solved using the computer software MATHEMATICA, making use of the *Solve* command, with the conditions that α should be real and should lie between 0 and L.

Putting $\beta=0.78L$ and $\alpha=0.227596L$ into Eq. (5), we get the coefficients $c_0, c_1, \ldots, c_6$ in Eq. (4) and thus the assumed polynomial variation $\phi(x)$ is now given by

$$\phi(x)=1.05566-0.969912x+0.0383512x^4-0.00920429x^5+0.000613619x^6 \tag{13}$$

Thus, solving the set of linear homogeneous equations, given by Eq. (11), we get $\{y\}^{(1)}$ as given in Appendix A. The final expressions for the mass and stiffness variations are given by

$$m(x)=(1+0.0259302x)a_0 \tag{14}$$

$$EI(x)=(1.14692+0.117428x-0.00345973x^2-0.006081x^3+0.000483766x^4+0.0000120047x^5)\omega^2 a_0 \tag{15}$$

The assumed mode shape function $\phi(x)$, given by Eq. (13), is shown in Fig. 1, along with some other mode shape functions which are obtained for different values of the parameter β. The corresponding variation of the obtained mass and stiffness of the beam is portrayed in Fig. 2. While plotting the mass and stiffness variations we assumed $\omega=5.83212$ rad/s and $a_0=1.8816$. We can observe that as β moves away from the actual fundamental mode shape of a uniform free–free beam ($\beta=0.775849L$) the variation of the mass and stiffness distributions, over the length of the beam, becomes higher.

This shows the existence of a class of non-uniform free–free beam, given by the above variations of mass (Eq. (14)) and stiffness (Eq. (15)), which has an exact solution given by Eq. (13). It is to be noted that in obtaining these solutions, we have assumed the value of one of the internal nodes β. Thus, for different values of this parameter, we will have different classes of non-uniform free–free beam with a closed-form solution, having linear mass distribution. Therefore, we can conclude that there exists an infinite number of non-uniform free–free beams, having linear mass distribution, which has a closed-form solution to its governing differential equation. Instead of solving the typically forward problem of finding a solution for a given beam, we have solved the inverse problem of finding the beam given a solution. We assumed the mode shape for a non-uniform free–free beam, along with some arbitrary constants, and determined the mass and stiffness variations for the beam. This inverse problem approach leads to this closed-form solution.

Thus, if a non-uniform free–free beam exists, whose mass and stiffness distributions are given by Eqs. (14) and (15), respectively, then the beam will vibrate with a fundamental frequency ω and fundamental mode shape given by Eq. (13). If such a beam really exists, it would interesting to calculate its dimensions for practical applications. For this we consider a non-uniform free–free beam with rectangular cross-section, whose height and breadth variations are given by $h(x)$ and $b(x)$, respectively. We already know $m(x)=\rho b(x)h(x)$ and $EI(x)=Eb(x)h(x)^3/12$, where ρ is the uniform material density and E is the elastic modulus of the beam. Knowing the variations of $m(x)$ and $EI(x)$, the height $h(x)$ and breadth $b(x)$ can be easily calculated as

$$h(x)=\sqrt{\frac{12\rho EI(x)}{Em(x)}} \tag{16}$$

$$b(x)=\sqrt{\frac{Em(x)^3}{12\rho^3 EI(x)}} \tag{17}$$

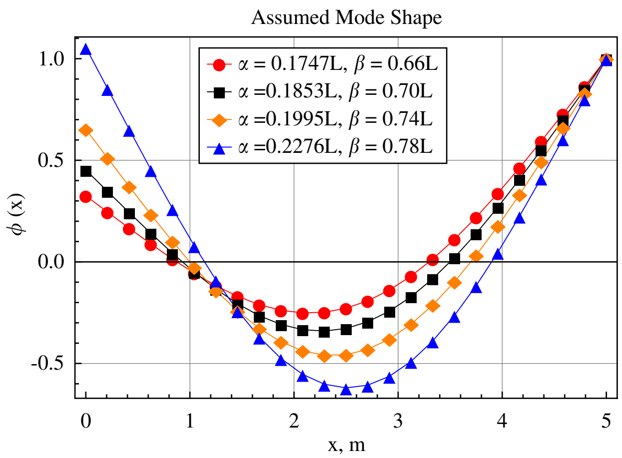

Fig. 1. The assumed mode shape $\phi(x)$, for the case of linear mass variation.

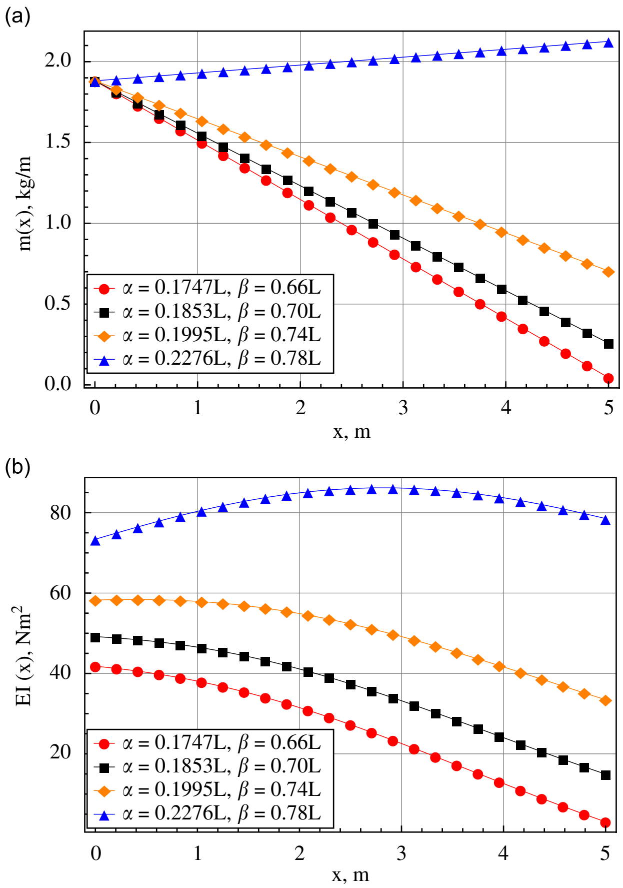

Fig. 2. Variation of the beam properties, for different locations of the internal nodes, corresponding to the case of linear mass distribution: (a) mass per unit length and (b) flexural stiffness.

For our case, we take length $L=5$ m, uniform material density $\rho = 7840\ \mathrm{kg/m^3}$ and elastic modulus $E = 2\times 10^{11}$ Pa. The height and breadth variations obtained for the different mass $m(x)$ and stiffness $EI(x)$ variations shown in Fig. 2 are portrayed by the three-dimensional plots shown in Fig. 3. For plotting purposes, the origin is taken as the centre of the cross-section at the base in Fig. 3. We can see that these are physically feasible beams which could be manufactured using CNC machining methods.

2.2. *Free-free beam with quadratic mass distribution (p=2)*

For this case, the mass and stiffness variations for the beam is given by

$$m(x) = a_0 + a_1 x + a_2 x^2 \tag{18}$$

$$EI(x) = b_0 + b_1 x + b_2 x^2 + b_3 x^3 + b_4 x^4 + b_5 x^5 + b_6 x^6 \tag{19}$$

Eq. (18) can be rewritten as

$$m(x) = a_0 + a_1 (x + \gamma_1 x^2) \tag{20}$$

where γ_1 is an arbitrary constant which gives the ratio of a_2/a_1. We put the expressions for $m(x)$ and $EI(x)$, given by Eqs. (20) and (19), and $\phi(x)$, given by Eq. (4), into Eq. (2), resulting in a polynomial expression with highest term x^8 and then set the coefficients of the various powers of x up to 8 to zero. Thus, yielding a set of nine linear homogeneous equations in nine unknowns

$$\mathbf{A}^{(2)} \mathbf{y}^{(2)} = \mathbf{0} \tag{21}$$

where the matrix $\mathbf{A}^{(2)}$ is given by Eq. (A.2) and the vector $\mathbf{y}^{(2)} = \{a_0, a_1, b_0, b_1, b_2, b_3, b_4, b_5, b_6\}^T$. Again, in order to have a non-trivial solution, the determinant of matrix $\mathbf{A}^{(2)}$ must be zero, leading to a complicated equation in α, β, γ_1 and ω, of the form $F_2(\alpha, \beta, \gamma_1)\omega^4 = 0$, where F_2 is a complicated polynomial expression in β, α and γ_1. This means that either $F_2(\alpha, \beta, \gamma_1) = 0$ or $\omega^4 = 0$. But always fundamental frequency $\omega > 0$, thus yielding

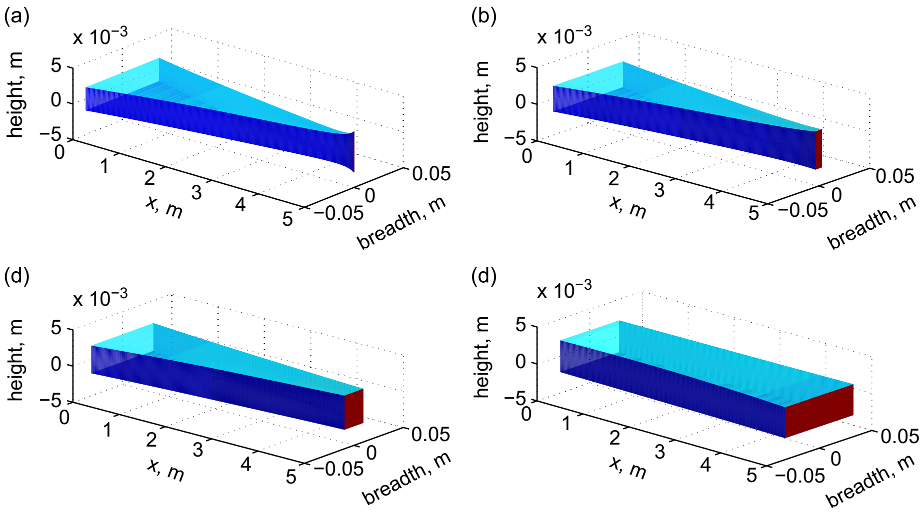

Fig. 3. Height and breadth variations for a free–free beam, corresponding to the mass and stiffness variations shown in Fig. 2, for different locations of the internal nodes: (a) for $\alpha=0.1747L$ and $\beta=0.66L$; (b) for $\alpha=0.1853L$ and $\beta=0.70L$; (c) for $\alpha=0.1995L$ and $\beta=0.74L$; and (d) for $\alpha=0.2276L$ and $\beta=0.78L$.

$$F_2(\alpha,\beta,\gamma_1)=0 \tag{22}$$

In order to solve Eq. (22), two of the three parameters have to specified. In this case, we will assume the value of one of the arbitrary nodes β and the parameter γ_1, and determine the other node α with respect to the specified values. The value of the known node is taken at $x=\beta=0.79L$ and the other parameter is taken as $\gamma_1=1.5$. Thus, solving Eq. (22) for α, the only real value that we get within the domain $0<\alpha<L$ is $\alpha=0.233026L$. Eq. (22) is solved using the computer software MATHEMATICA, making use of the *Solve* command, with the conditions that α should be real and should lie between 0 and L.

Putting $\gamma_1=1.5$, $\beta=0.79L$ and $\alpha=0.233026L$, into Eq. (5), we get the assumed polynomial variation $\phi(x)$ as

$$\phi(x)=1.17965-1.06057x+0.0409855x^4-0.00983651x^5+0.000655767x^6 \tag{23}$$

Thus, solving the set of linear homogeneous equations, given by Eq. (21), we get $\{y\}^{(2)}$ as given in Appendix A. The final expressions for the mass and stiffness variations are given by

$$m(x)=(1+0.0104126x+0.0156189x^2)a_0 \tag{24}$$

$$EI(x)=(1.19925+0.124466x+0.0030669x^2-0.00543588x^3+0.000480748x^4-0.000045796x^5+5.78476^{-6}x^6)\omega^2a_0 \tag{25}$$

The assumed mode shape function $\phi(x)$, given by Eq. (23), is shown in Fig. 4, along with some other mode shape functions which are obtained by using different values of the parameter β and $\gamma_1=1.5$. The corresponding variations of the obtained mass and stiffness of the beam have been portrayed in Fig. 5. While plotting we assumed $\omega=5.83212$ rad/s and $a_0=1.8816$. Here also we can observe that as the assumed mode shape moves away from the actual fundamental mode shape of the uniform free–free beam ($\beta=0.775849L$), the variation of the mass and stiffness distributions, over the length of the beam, becomes higher.

This shows the existence of another class of non-uniform free–free beam, given by the above variations of mass (Eq. (24)) and stiffness (Eq. (25)), which has an exact solution given by Eq. (23). It is to be noted that in obtaining these solutions, we have assumed the values of the parameter γ_1, and one of the internal nodes β.

Thus, if a non-uniform free–free beam exists, whose mass and stiffness distributions are given by Eqs. (24) and (25), respectively, then the beam will vibrate with a fundamental frequency ω, and fundamental mode shape given by Eq. (23). Similarly as before, the height and breadth variations of the rectangular cross-section of such a beam can be calculated by Eqs. (16) and (17). Using the same values of length, material density and elastic modulus, the height and breadth variations obtained for the different mass $m(x)$ and stiffness $EI(x)$ variations shown in Fig. 5, are portrayed by the three-dimensional plots shown in Fig. 6.

2.3. Free-free beam with cubic mass distribution ($p=3$)

For this case, the mass and stiffness variations for the beam is given by

$$m(x)=a_0+a_1x+a_2x^2+a_3x^3 \tag{26}$$

$$EI(x)=b_0+b_1x+b_2x^2+b_3x^3+b_4x^4+b_5x^5+b_6x^6+b_7x^7 \tag{27}$$

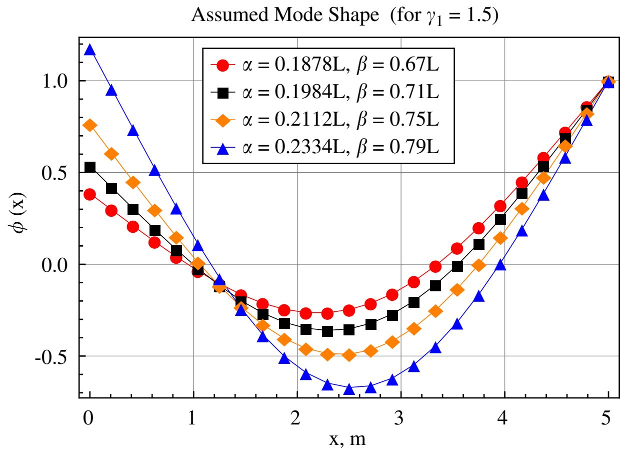

Fig. 4. The assumed mode shape $\phi(x)$, for the case of quadratic mass variation, using $\gamma_1 = 1.5$.

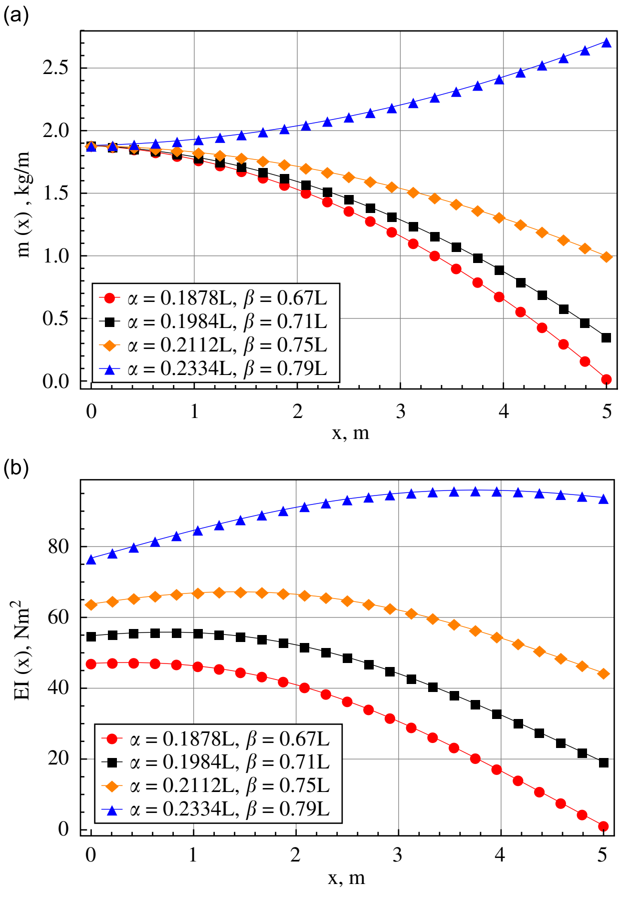

Fig. 5. Variation of the beam properties, for different locations of the internal nodes, corresponding to the case of quadratic mass distribution, using $\gamma_1 = 1.5$: (a) mass per unit length and (b) flexural stiffness.

Eq. (26) can be rewritten as

$$m(x) = a_0 + a_1\left(x + \gamma_1 x^2 + \gamma_2 x^3\right) \tag{28}$$

where γ_1 and γ_2 are arbitrary constants giving the ratios a_2/a_1 and a_3/a_1, respectively. Putting these expressions for $m(x)$ and $EI(x)$, given by Eqs. (28) and (27), and $\phi(x)$, given by Eq. (4), into Eq. (2), we get a polynomial equation with highest term

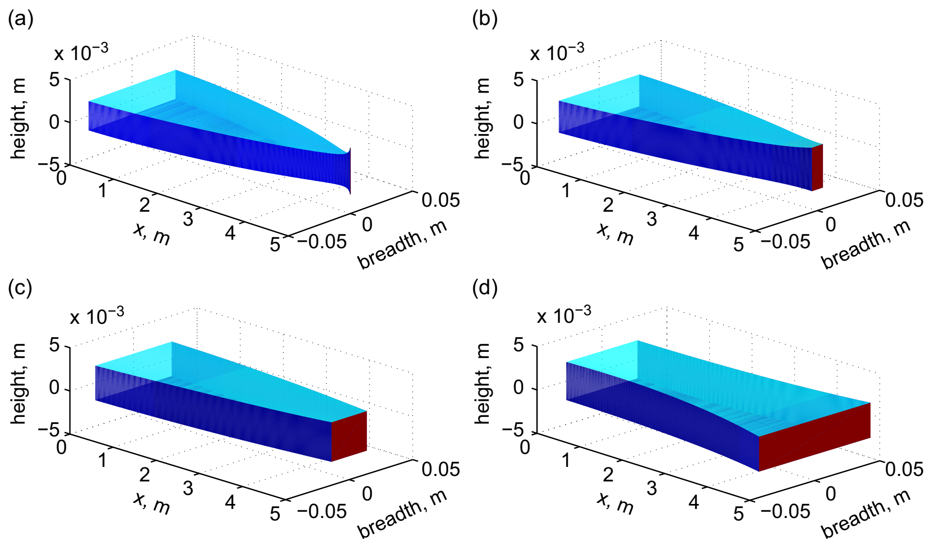

Fig. 6. Height and breadth variations for a free–free beam, corresponding to the mass and stiffness variations shown in Fig. 5, for different locations of the internal nodes: (a) for $\alpha=0.1878L$ and $\beta=0.67L$; (b) for $\alpha=0.1984L$ and $\beta=0.71L$; (c) for $\alpha=0.2112L$ and $\beta=0.75L$; and (d) for $\alpha=0.2334L$ and $\beta=0.79L$.

of x^9. We set the coefficients of the various powers of x to zero. Thus, yielding a set of ten linear homogeneous equations in ten unknowns.

$$\mathbf{A}^{(3)}\mathbf{y}^{(3)}=\mathbf{0} \tag{29}$$

where the matrix $\mathbf{A}^{(3)}$ is given by Eq. (A.3) and the vector $\mathbf{y}^{(3)}=\{a_0,a_1,b_0,b_1,b_2,b_3,b_4,b_5,b_6,b_7\}^T$. Once again, in order to have a non-trivial solution, the determinant of matrix $\mathbf{A}^{(3)}$ must be zero, leading to a complicated equation in $\alpha,\beta,\gamma_1,\gamma_2$ and ω, of the form $F_3(\alpha,\beta,\gamma_1,\gamma_2)\omega^4=0$, where F_3 is a complicated polynomial expression in β, α, γ_1 and γ_2. This means that either $F_3(\alpha,\beta,\gamma_1,\gamma_2)=0$ or $\omega^4=0$. But always fundamental frequency $\omega>0$, thus yielding

$$F_3(\alpha,\beta,\gamma_1,\gamma_2)=0 \tag{30}$$

In order to solve Eq. (30), three of the four parameters have to specified. In this case, we will assume the value of one of the arbitrary nodes β and the parameters γ_1 and γ_2, and determine the other node α with respect to the specified values. The value of the known node is taken at $x=\beta=0.8L$, and the other parameters are taken as $\gamma_1=1.5$ and $\gamma_2=1.2$. Thus, solving Eq. (30) for α, the only real value that we get within the domain $0<\alpha<L$ is $\alpha=0.235609L$.

Putting $\gamma_1=1.5$, $\gamma_2=1.2$, $\beta=0.8L$ and $\alpha=0.225609L$, into Eq. (5), we get the assumed polynomial variation $\phi(x)$ as

$$\phi(x)=1.29455–1.15174x+0.0437132x^4–0.0104912x^5+0.000699412x^6 \tag{31}$$

Thus, solving the set of linear homogeneous equations, given by Eq. (29), we get $\{y\}^{(3)}$ as given in Appendix A. The final expressions for the mass and stiffness variations are given by

$$m(x)=(1+0.00408112x+0.00612169x^2+0.00489735x^3)a_0 \tag{32}$$

$$EI(x)=(1.23394+0.129314x+0.0028805x^2–0.00408812x^3+0.000668882x^4–0.0000370153x^5–0.0000100998x^6+1.48405^{-6}x^7)\omega^2a_0 \tag{33}$$

The assumed mode shape function $\phi(x)$, given by Eq. (31), is shown in Fig. 7, along with some different mode shape functions which are obtained for different values of the parameter β, and $\gamma_1=1.5$ and $\gamma_2=1.2$. The corresponding variations of the obtained mass and stiffness of the beam have been portrayed in Fig. 8. While plotting we assumed $\omega=5.83212$ rad/s and a_0=1.8816. Once again, we observe that as the assumed mode shape moves away from the actual fundamental mode shape of a uniform free–free beam ($\beta=0.775849L$), the variation of the mass and stiffness distributions, over the length of the beam, becomes higher.

This shows the existence of another class of non-uniform free–free beam, given by the above variations of mass (Eq. (32)) and stiffness (Eq. (33)), which has an exact solution given by Eq. (31). It is to be noted that in obtaining these solutions, we have assumed the values of the parameters γ_1 and γ_2, and one of the nodes β.

Thus, if a non-uniform free–free beam exists, whose mass and stiffness distributions are given by Eqs. (32) and (33), respectively, then the beam will vibrate with a fundamental frequency ω and fundamental mode shape given by Eq. (31). Once again, the height and breadth variations of such a beam can be calculated by Eqs. (16) and (17). Using the same values of length, material density and elastic modulus, the height and breadth variations obtained for the different mass $m(x)$ and stiffness $EI(x)$ variations shown in Fig. 8 are portrayed by the three-dimensional plots shown in Fig. 9.

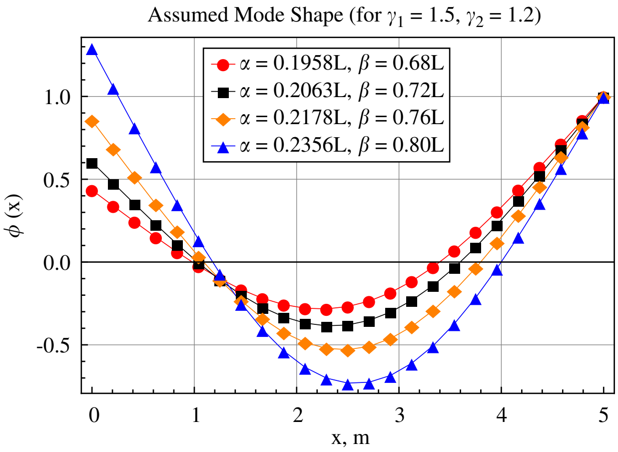

Fig. 7. The assumed mode shape $\phi(x)$, for the case of cubic mass variation, using $\gamma_1 = 1.5$ and $\gamma_2 = 1.2$.

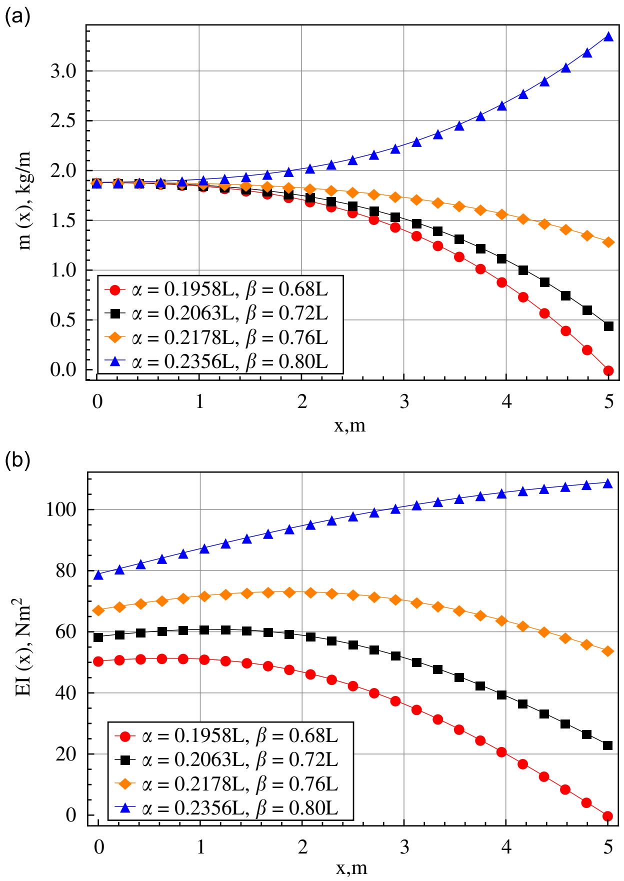

Fig. 8. Variation of the beam properties, for different locations of the internal nodes, corresponding to the case of cubic mass distribution, using $\gamma_1 = 1.5$ and $\gamma_2 = 1.2$: (a) mass per unit length and (b) flexural stiffness.

In most engineering structures, the mass distributions are generally of the types discussed above. But the theory can be extended to any order of polynomial for the mass distribution $m(x)$. Suppose that the polynomial order for $m(x)$ is given by p, then the corresponding stiffness distribution $EI(x)$ will be a $(p+4)$th-order polynomial. The coefficients of $m(x)$ (for any $p>3$) can always be rewritten in terms of a_0, a_1, $\gamma_1, \gamma_2, \ldots, \gamma_{p-1}$, where $\gamma_1 = a_2/a_1$, $\gamma_2 = a_3/a_1, \ldots, \gamma_{p-1} = a_p/a_1$. If we take the expressions for $m(x)$ and $EI(x)$, and the assumed polynomial, given by Eq. (4), and put them into the governing differential equation (Eq. (2)), we will get a polynomial equation in x. If this polynomial has to be satisfied for all values of x, then the coefficient of the various powers of x must be set to zero, leading to a set of $(p+7)$ linear homogeneous equations in $(p+7)$

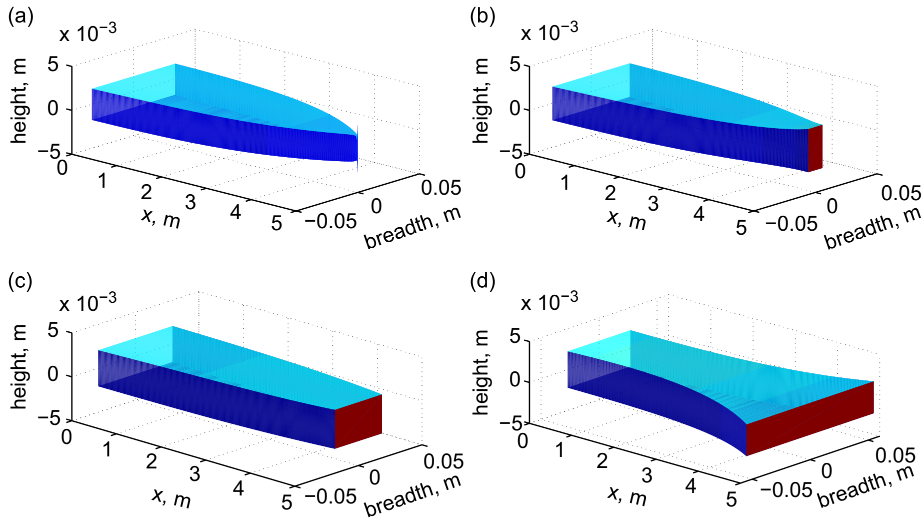

Fig. 9. Height and breadth variations for a free–free beam, corresponding to the mass and stiffness variations shown in Fig. 8, for different locations of the internal nodes: (a) for $\alpha = 0.1958L$ and $\beta = 0.68L$; (b) for $\alpha = 0.2063L$ and $\beta = 0.72L$; (c) for $\alpha = 0.2178L$ and $\beta = 0.76L$; and (d) for $\alpha = 0.2356L$ and $\beta = 0.80L$.

unknowns $(a_0, a_1, b_0, b_1, \ldots b_{p+4})$. Arguing in the same manner as shown in the three different cases, we can say that if the set of linear equations has to have a solution, then the determinant of the coefficient matrix must be equal to zero, leading to a complicated equation in terms of the fundamental frequency ω, the arbitrary parameters $\gamma_1, \ldots, \gamma_{p-1}$, and the internal nodes α and β, of the form $F(\alpha, \beta, \gamma_1, \ldots, \gamma_{p-1})\omega^4 = 0$. This means that either $F(\alpha, \beta, \gamma_1, \ldots, \gamma_{p-1}) = 0$ or $\omega^4 = 0$. But always fundamental frequency $\omega > 0$, thus yielding

$$F(\alpha, \beta, \gamma_1, \ldots, \gamma_{p-1}) = 0 \tag{34}$$

In order to solve Eq. (34), $(p+1)$ of the $(p+2)$ parameters have to specified, and the $(p+2)$th parameter needs to be determined in terms of the prescribed values. Once this is done, we can easily get the values of c_i's from Eq. (5), using which we can arrive at the expression for the assumed polynomial for that particular case. Once we have all the values, we can solve the set of $(p+7)$ linear homogeneous equations and get the values of the unknowns $(a_1, b_0, b_1, \ldots b_{p+4})$ in terms of the fundamental frequency ω and the arbitrary constant a_0, which will give us the final expressions for the mass $m(x)$ and stiffness $EI(x)$ variations.

2.4. Free–free beam with external elastic constraints at the internal nodes

When we introduce external elastic constraints at the internal node locations, the boundary conditions at the internal nodes will contain the flexural stiffness of the beam. Hence, the assumed mode shape would be a function of the flexural stiffness of the beam at the points of the internal node. If we now assume polynomial variations for the mass and stiffness variations and put them into the governing differential equation, along with the assumed polynomial, and make the coefficients of the various powers of x to go to zero, we will get a system of nonlinear equations, which does not have any analytical solution. Thus, we take a different approach in order to solve this problem.

We consider the whole beam to be made up of three different sections as shown in Fig. 10. The flexural stiffness is considered uniform in each section and is given by EI_i (where $i = 1, 2, 3$), $m_i(x)$ denotes the mass per unit length variation for the ith section, $\phi_i(x)$ denotes the mode shape variation of the ith section, α and β denote the internal node locations from the origin at $x=0$ on the left hand side of the beam, k_{t1} and k_{t2} denotes the spring constants of the two translational springs, and k_{r1} and k_{r2} denote the torsional spring constants of the two rotational springs at the internal nodes α and β, respectively. The boundary conditions for the non-uniform free–free beam, shown in Fig. 10, are given by

$$\begin{gathered}
\phi''_1(0) = 0, \quad \phi_1'''(0) = 0, \quad \phi_1(\alpha) = 0, \quad \phi_2(\alpha) = 0, \quad \phi'_1(\alpha) = \phi'_2(\alpha), \\
EI_1\phi''_1(\alpha) = -k_{r1}\phi'_1(\alpha) + EI_2\phi''_2(\alpha), \quad EI_1\phi'''_1(\alpha) = EI_2\phi'''_2(\alpha), \\
\phi_2(\beta) = 0, \quad \phi_3(\beta) = 0, \quad \phi'_2(\beta) = \phi'_3(\beta) \\
EI_2\phi''_2(\beta) = -k_{r2}\phi'_2(\beta) + EI_3\phi''_3(\beta), \quad EI_2\phi'''_2(\beta) = EI_3\phi'''_3(\beta), \\
\phi''_3(L) = 0, \quad \phi'''_3(L) = 0, \quad \phi_3(L) = 1
\end{gathered} \tag{35}$$

Upon careful observation of the boundary conditions, given by Eq. (35), one can immediately conclude that the translational springs play no role in the boundary conditions because of the displacements being zero at the internal node locations. We

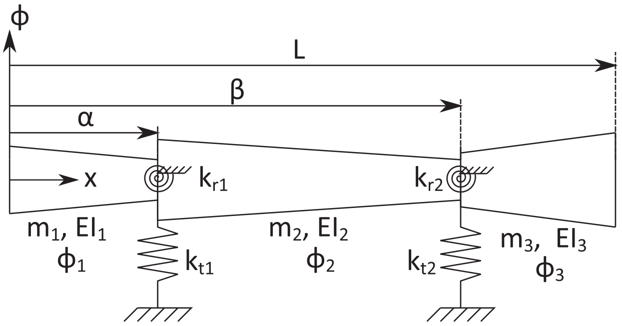

Fig. 10. Schematic of a non-uniform free–free beam with external elastic constraints at the internal nodes.

now assume the mode shapes, ϕ_i's, at the three different sections, as simple polynomials of varying degrees of x, as follows:

$$\phi_1(x)=\sum_{i=0}^{5}a_i\left(\frac{x}{L}\right)^i,\quad \phi_2(x)=\sum_{i=0}^{6}b_i\left(\frac{x}{L}\right)^i,\quad \phi_3(x)=\sum_{i=0}^{5}c_i\left(\frac{x}{L}\right)^i \tag{36}$$

The reason for choosing the order of the polynomials for each of the three mode shapes will become clear with the subsequent mathematical formulations. Putting Eq. (36) into Eq. (35), we will have 15 linear homogeneous equations in nineteen variables $(a_0,\ldots,a_5,b_0,\ldots,b_6,c_0,\ldots,c_5)$, solving which we will get the expression for 15 variables $(a_0,\ldots,a_4,b_0,\ldots,b_4,c_0,\ldots,c_4)$ in terms of the beam length L, internal node locations α and β, the flexural stiffness EI_i's of the three sections and four unknown constants a_5,b_5,b_6 and c_5. Thus, we can arrive at an expression for the assumed mode shapes ϕ_i's using Eq. (36). Now, the governing differential equation for each section of the beam is given by

$$EI_i\phi_i^{IV}(x)-m_i(x)\omega^2\phi_i(x)=0\quad(i=1,2,3) \tag{37}$$

where ω denotes the fundamental frequency of the non-uniform free–free beam. Once the mode shape ϕ_i's are determined, we can derive the mass variation of each section as follows:

$$m_i(x)=\frac{EI_i\phi_i^{IV}(x)}{\omega^2\phi_i(x)} \tag{38}$$

Now, due to the presence of the internal nodes, we have the conditions $\phi_1(\alpha)=\phi_2(\alpha)=\phi_2(\beta)=\phi_3(\beta)=0$. Hence, the mass variations will encounter singularities at the internal node locations because of the presence of the mode shape function $\phi_i(x)$ in the denominator of Eq. (38). To avoid these singularities, we impose the additional constraint such that the numerator of Eq. (38) should also be zero at the internal node locations. Thus, by the L'Hospital's rule, we will have a zero by zero condition at the internal nodes, which removes the singularity in the mass variation at these points. Thus, imposing the numerator of $m_1(x)$ to be zero at $x=\alpha$, numerator of $m_2(x)$ to be zero at $x=\alpha$ and $x=\beta$, and numerator of $m_3(x)$ to be zero at $x=\beta$, we will get four linear homogeneous equations in four variables (a_5,b_5,b_6,c_5), solving which we will get the final expressions for the unknown constants a_5,b_5,b_6 and c_5. We have now solved for all the unknown constants, which enable us to get the final expressions for the mode shapes and mass variations of each section, using Eqs. (36) and (38), respectively.

As an example, we take a non-uniform free–free beam where the flexural stiffness variations of the three sections are given by 400 Nm^2, 200 Nm^2 and 300 Nm^2, respectively. The length of the beam is taken as 5 m and the torsional stiffness constants, k_{r1} and k_{r2}, of the rotational springs are taken as 100 Nm/rad and 150 Nm/rad, respectively. The fundamental frequency ω is assumed to be 10 rad/s. Fig. 11 shows the total mode shape variation $\phi(x)$ of the beam, for different positions of the internal nodes at $x=\alpha$ and $x=\beta$, where the values of α are taken as $0.20L$, $0.25L$, $0.30L$, and $0.35L$ and the corresponding values of β are taken as $0.65L, 0.70L, 0.75L,$ and $0.8L$. Fig. 12 shows the mass per unit length variations of the three different sections of the non-uniform free–free beam, corresponding to the mode shapes shown in Fig. 11. Similarly as before, the height and breadth variations of the rectangular cross-section of such a beam can be calculated by Eqs. (16) and (17). Using the same values of length ($L=5$ m), material density ($\rho=7840\ \text{kg/m}^3$) and elastic modulus ($E=2\times10^{11}\ \text{N/m}^2$), the height and breadth variations obtained for the different mass $m(x)$ variations shown in Fig. 12 are portrayed by the three-dimensional plots shown in Fig. 13.

This shows the existence of a class of non-uniform free–free beam, having external elastic constraints at the internal nodes, given by the mass variations shown in Fig. 12, which has an exact solution given by the mode shapes shown in Fig. 11. It is to be noted that in obtaining these solutions, we have assumed the value of the internal nodes at $x=\alpha$ and $x=\beta$, and other parameters like length, flexural stiffness, spring constants. Thus, for different values of these parameters, we will have different classes of non-uniform free–free beam with a fundamental closed-form solution to its governing differential equation, having external elastic constraints at the internal nodes.

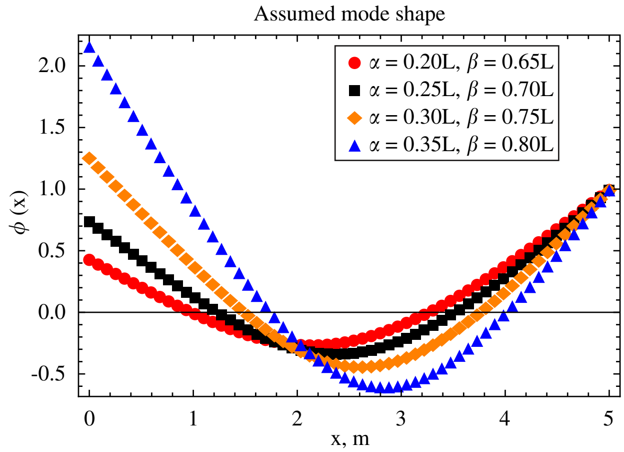

Fig. 11. The assumed mode shape $\phi(x)$ of a non-uniform free–free beam, having external elastic constraints at the internal nodes, corresponding to different internal node locations.

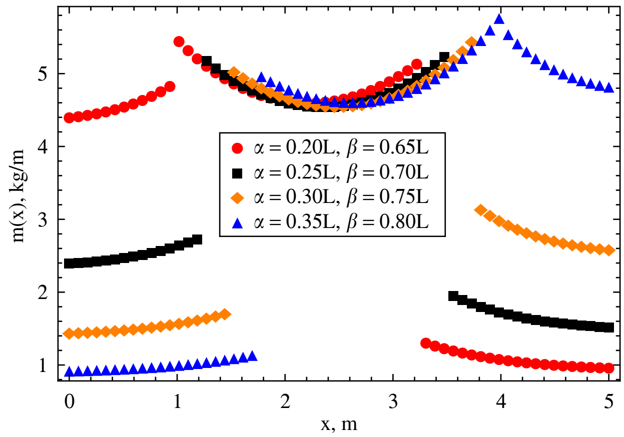

Fig. 12. Mass variation of the non-uniform free–free beam, having external elastic constraints at the internal nodes, corresponding to the mode shape variations shown in Fig. 11.

3. Derived mass and stiffness functions used as test functions for p-version FEM

The finite element method is one of the most popular methods used for the vibration analysis of non-uniform beams. Most of the early works have used the Hermite cubic polynomial as shape functions, which is known as the h-version finite element method [33]. This method works well for uniform beams, but for non-uniform beams a large number of elements are required for the convergence of results. Hence in later years new types of finite element methods were developed which uses only one element like the p-version [34], Fourier-p super element [35] and spectral methods [36].

The mass $m(x)$ and stiffness distributions $EI(x)$ obtained in Sections 2.1–2.3 can be used as benchmark solutions for validating the different numerical methods developed for non-uniform beams. In our case, we will use the derived results for the validation of the p-version finite element method. Here only one element is used for the whole beam. This version is used because it can handle non-uniform variations of mass and flexural stiffness, and also due to reduced order of the eigenvalue problem.

We take the derived $m(x)$ and $EI(x)$ variations, shown in Fig. 2, corresponding to the assumed mode shapes for the case of linear mass variation, shown in Fig. 1, and put them into the FEM formulation to obtain the fundamental frequency and mode shape. We assumed $\omega = 5.83212$ and $a_0 = 1.8816$. The obtained numerical results are compared with the assumed fundamental frequency ω and mode shape $\phi(x)$. The obtained frequency matches up to the fifth place of decimal for $\beta = 0.66L, 0.70L, 0.74L$ and $0.78L$. The mode shape comparisons are shown in Fig. 14. Since the $m(x)$ and $EI(x)$ variations are simple polynomial functions, we can observe that the rate of convergence is very fast. The order of polynomial basis needed for convergence is only six. Thus, we observe that the test functions, derived for the different types of beams, give back the same fundamental frequency and mode shape that we had assumed. Once the numerical code is verified for the fundamental mode, we can easily get the higher mode frequencies and mode shapes using the same. The derived test functions can also be used to verify the implementation of Rayleigh–Ritz and Galerkin method.

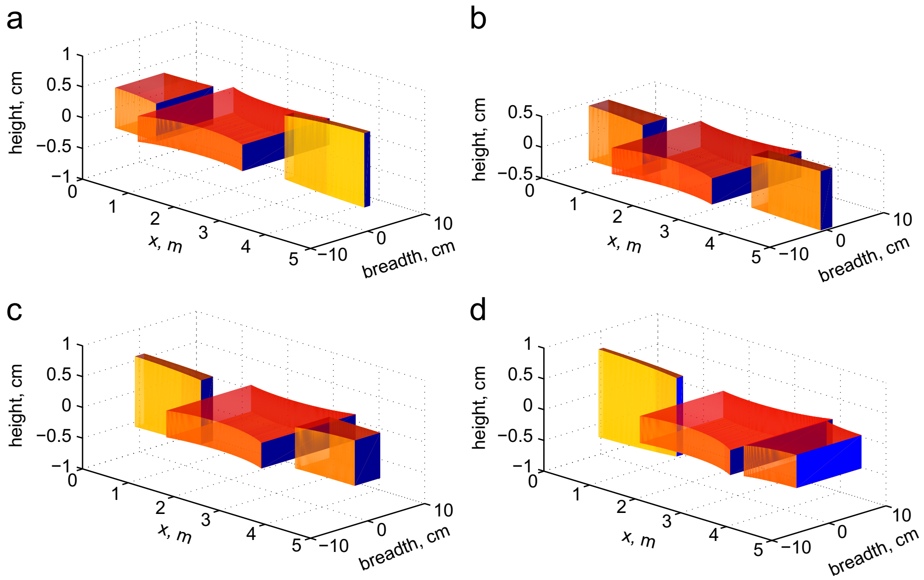

Fig. 13. Height and breadth variations for a non-uniform free–free beam, having external elastic constraints at the internal nodes, corresponding to the mass variations shown in Fig. 12, for different locations of the internal nodes: (a) for $\alpha=0.20L$ and $\beta=0.65L$; (b) for $\alpha=0.25L$ and $\beta=0.70L$; (c) for $\alpha=0.30L$ and $\beta=0.75L$; and (d) for $\alpha=0.35L$ and $\beta=0.80L$.

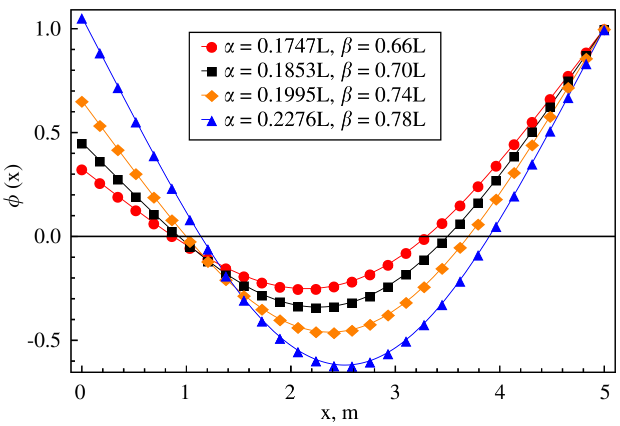

Fig. 14. Comparison of the assumed fundamental mode shapes and mode shapes obtained from p-FEM, for the case of linear mass variations for different values of the node β. The markers indicate the fundamental mode shapes obtained from the p-FEM, the continuous lines indicate the assumed fundamental mode shapes.

4. Conclusion

In this paper, we have shown that there exists a certain class of non-uniform Euler–Bernoulli beam, having free–free boundary condition, which has a closed-form polynomial solution to its homogenous governing differential equation. We assume a certain mode shape function $\phi(x)$, which satisfies all the given boundary conditions, from which we derived the mass distribution $m(x)$ and flexural stiffness $EI(x)$ of the beam. These derived properties are simple polynomial functions which depend on the fundamental frequency ω and the arbitrary constant a_0, for prescribed values of the parameters $\gamma_1, \gamma_2, \ldots, \gamma_{p-1}$, and internal nodes α and β. So essentially, given a certain fundamental frequency ω, we can tailor the properties of the non-uniform free–free beam. This might be useful for some practical design applications where the fundamental frequency might be required to assume a desired value or if the location of the internal nodes needs to be shifted. We have also considered a special case where, at the internal nodes, the external elastic constraints are present, where we considered two translational and two rotational constraints at the internal nodes, and consequently divided the beam into three sections having uniform stiffness variation, but variable mass per unit lengths. We assumed simple polynomial mode shapes for each of the three sections and derived them using all the relevant boundary conditions of the non-uniform free–free beam, which leads to another class of closed-form solutions and also enables us to tailor the internal node locations, given a certain fundamental frequency and other beam parameters. But most importantly, these closed-form solutions serve as benchmark solutions for the validation of numerical or approximate methods used for non-uniform beam vibration analysis. Hence, the derived properties $m(x)$ and $EI(x)$ have been used to validate the p-version finite element code for non-uniform free–free beam, thus proving their usefulness as test functions.

Appendix A. Equation matrices and their solutions

$$\mathbf{A}^{(1)} = \begin{pmatrix} -\omega^2 c_0 & 0 & 24c_4 & 12c_3 & 4c_2 & 0 & 0 & 0 \\ -\omega^2 c_1 & -\omega^2 c_0 & 120c_5 & 72c_4 & 36c_3 & 12c_2 & 0 & 0 \\ -\omega^2 c_2 & -\omega^2 c_1 & 360c_6 & 240c_5 & 144c_4 & 72c_3 & 24c_2 & 0 \\ -\omega^2 c_3 & -\omega^2 c_2 & 0 & 600c_6 & 400c_5 & 240c_4 & 120c_3 & 40c_2 \\ -\omega^2 c_4 & -\omega^2 c_3 & 0 & 0 & 900c_6 & 600c_5 & 360c_4 & 180c_3 \\ -\omega^2 c_5 & -\omega^2 c_4 & 0 & 0 & 0 & 1260c_6 & 840c_5 & 504c_4 \\ -\omega^2 c_6 & -\omega^2 c_5 & 0 & 0 & 0 & 0 & 1680c_6 & 1120c_5 \\ 0 & -\omega^2 c_6 & 0 & 0 & 0 & 0 & 0 & 2160c_6 \end{pmatrix} \tag{A.1}$$

$$\mathbf{A}^{(2)} = \begin{pmatrix} -\omega^2 c_0 & 0 & 24c_4 & 12c_3 & 4c_2 & 0 & 0 & 0 & 0 \\ -\omega^2 c_1 & -\omega^2 c_0 & 120c_5 & 72c_4 & 36c_3 & 12c_2 & 0 & 0 & 0 \\ -\omega^2 c_2 & -\omega^2 (c_1 + c_0\gamma_1) & 360c_6 & 240c_5 & 144c_4 & 72c_3 & 24c_2 & 0 & 0 \\ -\omega^2 c_3 & -\omega^2 (c_2 + c_1\gamma_1) & 0 & 600c_6 & 400c_5 & 240c_4 & 120c_3 & 40c_2 & 0 \\ -\omega^2 c_4 & -\omega^2 (c_3 + c_2\gamma_1) & 0 & 0 & 900c_6 & 600c_5 & 360c_4 & 180c_3 & 60c_2 \\ -\omega^2 c_5 & -\omega^2 (c_4 + c_3\gamma_1) & 0 & 0 & 0 & 1260c_6 & 840c_5 & 504c_4 & 252c_3 \\ -\omega^2 c_6 & -\omega^2 (c_5 + c_4\gamma_1) & 0 & 0 & 0 & 0 & 1680c_6 & 1120c_5 & 672c_4 \\ 0 & -\omega^2 (c_6 + c_5\gamma_1) & 0 & 0 & 0 & 0 & 0 & 2160c_6 & 1440c_5 \\ 0 & -\omega^2 c_6\gamma_1 & 0 & 0 & 0 & 0 & 0 & 0 & 2700c_6 \end{pmatrix} \tag{A.2}$$

$$\mathbf{A}^{(3)} = \begin{pmatrix} -\omega^2 c_0 & 0 & 24c_4 & 12c_3 & 4c_2 & 0 & 0 & 0 & 0 & 0 \\ -\omega^2 c_1 & -\omega^2 c_0 & 120c_5 & 72c_4 & 36c_3 & 12c_2 & 0 & 0 & 0 & 0 \\ -\omega^2 c_2 & -\omega^2 (c_1 + c_0\gamma_1) & 360c_6 & 240c_5 & 144c_4 & 72c_3 & 24c_2 & 0 & 0 & 0 \\ -\omega^2 c_3 & -\omega^2 (c_2 + c_1\gamma_1 + c_0\gamma_2) & 0 & 600c_6 & 400c_5 & 240c_4 & 120c_3 & 40c_2 & 0 & 0 \\ -\omega^2 c_4 & -\omega^2 (c_3 + c_2\gamma_1 + c_1\gamma_2) & 0 & 0 & 900c_6 & 600c_5 & 360c_4 & 180c_3 & 60c_2 & 0 \\ -\omega^2 c_5 & -\omega^2 (c_4 + c_3\gamma_1 + c_2\gamma_2) & 0 & 0 & 0 & 1260c_6 & 840c_5 & 504c_4 & 252c_3 & 84c_2 \\ -\omega^2 c_6 & -\omega^2 (c_5 + c_4\gamma_1 + c_3\gamma_2) & 0 & 0 & 0 & 0 & 1680c_6 & 1120c_5 & 672c_4 & 336c_3 \\ 0 & -\omega^2 (c_6 + c_5\gamma_1 + c_4\gamma_2) & 0 & 0 & 0 & 0 & 0 & 2160c_6 & 1440c_5 & 864c_4 \\ 0 & -\omega^2 (c_6\gamma_1 + c_5\gamma_2) & 0 & 0 & 0 & 0 & 0 & 0 & 2700c_6 & 1800c_5 \\ 0 & -\omega^2 c_6\gamma_2 & 0 & 0 & 0 & 0 & 0 & 0 & 0 & 3300c_6 \end{pmatrix} \tag{A.3}$$

where c_i's are given by Eq. (5). The solutions of the Eqs. (11), (21) and (29), as mentioned in Sections 2.1–2.3, are given by

$$\mathbf{y}^{(1)} = \begin{pmatrix} a_0 \\ 0.0259302a_0 \\ 1.14692\omega^2 a_0 \\ 0.117428\omega^2 a_0 \\ -0.00345973\omega^2 a_0 \\ -0.006081\omega^2 a_0 \\ 0.000483766\omega^2 a_0 \\ 0.0000120047\omega^2 a_0 \end{pmatrix}, \quad \mathbf{y}^{(2)} = \begin{pmatrix} a_0 \\ 0.0104126a_0 \\ 1.19925\omega^2 a_0 \\ 0.124466\omega^2 a_0 \\ 0.0030669\omega^2 a_0 \\ -0.00543588\omega^2 a_0 \\ 0.000480748\omega^2 a_0 \\ -0.000045796\omega^2 a_0 \\ 5.78476^{-6}\omega^2 a_0 \end{pmatrix}, \quad \mathbf{y}^{(3)} = \begin{pmatrix} a_0 \\ 0.00408112a_0 \\ 1.23394\omega^2 a_0 \\ 0.129314\omega^2 a_0 \\ 0.0028805\omega^2 a_0 \\ -0.00408812\omega^2 a_0 \\ 0.000668882\omega^2 a_0 \\ -0.0000370153\omega^2 a_0 \\ -0.0000100998\omega^2 a_0 \\ 1.48405^{-6}\omega^2 a_0 \end{pmatrix} \tag{A.4}$$

where ω is the fundamental frequency and a_0 is any arbitrary constant.

References

[1] D. Platus, Aeroelastic stability of slender, spinning missiles, *Journal of Guidance, Control and Dynamics* 15 (1992) 144–151.
[2] W. Mermagen, C. Murphy, Flight mechanics of an elastic symmetric missile, *Journal of Guidance, Control and Dynamics* 24 (6) (2001) 1125–1132.
[3] S. Pradhan, P. Datta, Dynamic instability characteristics of a free–free missile structure under a controlled follower force, *Aircraft Engineering and Aerospace Technology: An International Journal* 78 (6) (2006) 509–514.

[4] T. Ohshima, Y. Sugiyama, Dynamic stability of free–free beam subjected to end rocket thrust and carrying a heavy payload at its nose, *2003 International Conference Physics and Control*, Vol. 4, IEEE, 2003, pp. 1115–1120.

[5] J. Wu, C. Ho, Analysis of wave-induced horizontal-and-torsion-coupled vibrations of a ship hull, *Journal of Ship Research* 31 (4) (1987) 235–252.

[6] H. Brody, The sweet spot of a baseball bat, *American Journal of Physics* 54 (1986) 640–643.

[7] H. Brody, Models of baseball bats, *American Journal of Physics* 58 (8) (1990) 756–758.

[8] K. Wang, A. Wong, C. Nguyen, VHF free–free beam high-Q micromechanical resonators, *Journal of Microelectromechanical Systems* 9 (3) (2000) 347–360.

[9] M. Demirci, C. Nguyen, Higher-mode free–free beam micromechanical resonators, *Proceedings of the 2003 IEEE International on Frequency Control Symposium and PDA Exhibition Jointly with the 17th European Frequency and Time Forum*, IEEE, 2003, pp. 810–818.

[10] Z. Davis, W. Svendsen, A. Boisen, Design, fabrication and testing of a novel MEMS resonator for mass sensing applications, *Microelectronic Engineering* 84 (5–8) (2007) 1601–1605.

[11] S. Caddemi, I. Calio, Exact closed-form solution for the vibration modes of the Euler–Bernoulli beam with multiple open cracks, *Journal of Sound and Vibration* 327 (3) (2009) 473–489.

[12] V. Stojanovic, P. Kozic, G. Janevski, Exact closed-form solutions for the natural frequencies and stability of elastically connected multiple beam system using Timoshenko and high-order shear deformation theory, Journal of Sound and Vibration 332 (3) (2013) 563–576.

[13] J. Rusin, P. Sniady, P. Sniady, Vibrations of double-string complex system under moving forces. Closed solutions, *Journal of Sound and Vibration* 330 (3) (2011) 404–415.

[14] Q. Gao, F. Wu, H. Zhang, W. Zhong, W. Howson, F. Williams, Exact solutions for dynamic response of a periodic spring and mass structure, *Journal of Sound and Vibration* 331 (2012) 1183–1190.

[15] S. Naguleswaran, Vibration of an Euler–Bernoulli beam of constant depth and with linearly varying breadth, *Journal of Sound and Vibration* 153 (3) (1992) 509–522.

[16] S. Naguleswaran, A direct solution for the transverse vibration of Euler–Bernoulli wedge and cone beams, *Journal of Sound and Vibration* 172 (3) (1994) 289–304.

[17] D. Zhou, Y. Cheung, The free vibration of a type of tapered beams, *Computer Methods in Applied Mechanics and Engineering* 188 (1) (2000) 203–216.

[18] I. Elishakoff, S. Candan, Apparently first closed-form solution for vibrating: *inhomogeneous beams*, *International Journal of Solids and Structures* 38 (19) (2001) 3411–3441.

[19] S. Candan, I. Elishakoff, Constructing the axial stiffness of longitudinally vibrating rod from fundamental mode shape, *International Journal of Solids and Structures* 38 (19) (2001) 3443–3452.

[20] R. Becquet, I. Elishakoff, Class of analytical closed-form polynomial solutions for guided-pinned inhomogeneous beams, *Chaos, Solitons & Fractals* 12 (8) (2001) 1509–1534.

[21] I. Elishakoff, Z. Guede, A remarkable nature of the effect of boundary conditions on closed-form solutions for vibrating inhomogeneous Bernoulli–Euler beams, *Chaos, Solitons & Fractals* 12 (4) (2001) 659–704.

[22] Z. Guede, I. Elishakoff, Apparently first closed-form solutions for inhomogeneous vibrating beams under axial loading, *Proceedings of the Royal Society of London. Series A*: *Mathematical, Physical and Engineering Sciences* 457 (2007) (2001) 623–649.

[23] Z. Guede, I. Elishakoff, A fifth-order polynomial that serves as both buckling and vibration mode of an inhomogeneous structure, *Chaos, Solitons & Fractals* 12 (7) (2001) 1267–1298.

[24] J. Storch, I. Elishakoff, Apparently first closed-form solutions of inhomogeneous circular plates in 200 years after Chladni, *Journal of Sound and Vibration* 276 (3–5) (2004) 1108–1114.

[25] I. Elishakoff, *Eigenvalues of Inhomogeneous Structures*: *Unusual Closed-form Solutions*, CRC Press, 2004.

[26] I. Elishakoff, D. Pentaras, Apparently the first closed-from solution of inhomogeneous elastically restrained vibrating beams, *Journal of Sound and Vibration* 298 (1) (2006) 439–445.

[27] I. Calio, I. Elishakoff, Can a trigonometric function serve both as the vibration and the buckling mode of an axially graded structure? *Mechanics Based Design of Structures and Machines* 32 (4) (2004) 401–421.

[28] I. Calio, I. Elishakoff, Closed-form trigonometric solutions for inhomogeneous beam-columns on elastic foundation, *International Journal of Structural Stability and Dynamics* 4 (1) (2004) 139–146.

[29] I. Calio, I. Elishakoff, Closed-form solutions for axially graded beam-columns, *Journal of Sound and Vibration* 280 (3) (2005) 1083–1094.

[30] R. Gilat, I. Calio, I. Elishakoff, Inhomogeneous beams possessing an exponential mode shape, *Mechanics Research Communications* 37 (4) (2010) 417–426.

[31] J. Neuringer, I. Elishakoff, Inhomogeneous beams that may possess a prescribed polynomial second mode, *Chaos, Solitons & Fractals* 12 (5) (2001) 881–896.

[32] L. Meirovitch, *Elements of Vibration Analysis*, Vol. 2, McGraw-Hill, New York, 1986.

[33] K.M. Udupa, T.K. Varadan, Hierarchical finite element method for rotating beams, *Journal of Sound and Vibration* 138 (3) (1990) 447–456.

[34] D.H. Hodges, M.J. Rutkowski, Free-vibration analysis of rotating beams by a variable-order finite-element method, *AIAA Journal* 19 (11) (1981) 1459–1466.

[35] J.B. Gunda, A.P. Singh, P.S. Chhabra, R. Ganguli, Free vibration analysis of rotating tapered blades using Fourier-*p* superelement, *Structural Engineering and Mechanics* 27 (2) (2007) 243–257.

[36] K.G. Vinod, S. Gopalakrishnan, R. Ganguli, Free vibration and wave propagation analysis of uniform and tapered rotating beams using spectrally formulated finite elements, *International Journal of Solids and Structures* 44 (18–19) (2007) 5875–5893.